

# Multi-scenario urban flood risk assessment by integrating future land use change models and hydrodynamic models

Qinke Sun<sup>1,2</sup>, Jiayi Fang<sup>1,2</sup>, Xuewei Dang<sup>3</sup>, Kepeng Xu<sup>1,2</sup>, Yongqiang Fang<sup>1,2</sup>, Xia Li<sup>1,2</sup>, Min Liu<sup>1,2</sup>

<sup>1</sup>School of Geographic Sciences, East China Normal University, Shanghai 200241, China

<sup>2</sup>Key Laboratory of Geographic Information Science (Ministry of Education), East China Normal University, Shanghai 200241, China

<sup>3</sup>Faculty of Geomatics, Lanzhou Jiaotong University, Lanzhou 730070, China

Correspondence to: Jiayi Fang (jyfang822@foxmail.com); Min Liu (mliu@geo.ecnu.edu.cn)

**Abstract.** Urbanization and climate change are the critical challenges in the 21<sup>st</sup> century. Flooding by extreme weather events and human activities can lead to catastrophic impacts in fast-urbanizing areas. However, high uncertainty in climate change and future urban growth limit the ability of cities to adapt to flood risk. This study presents a multi-scenario risk assessment method that couples the future land use simulation model (FLUS) and floodplain inundation model (LISFLOOD-FP) to simulate and evaluate the impacts of future urban growth scenarios with flooding under climate change (two representative concentration pathways (RCPs 2.6 and 8.5)). By taking ~~Shanghai~~-coastal city of Shanghai as an example, we then quantify the role of urban planning policies in future urban development to compare urban development under multiple policy scenarios (Business as usual, ~~BU~~; Growth as planned, ~~GP~~; Growth as eco-constraints, ~~GE~~). Geospatial databases related to anthropogenic flood protection facilities, land subsidence, and storm surge are developed and used as inputs to the LISFLOOD-FP model to estimate flood risk under various urbanization and climate change scenarios. The results show that urban growth under the three scenario models manifests significant differences in expansion trajectories, influenced by key factors such as infrastructure development and policy constraints. Comparing the urban inundation results for the RCP2.6 and RCP8.5 scenarios, the urban inundation area under the growth as eco-constraints~~GE~~ scenario is less than that under the business as usual~~BU~~ scenario, but more than that under the growth as planned~~GP~~ scenario. We also find that urbanization tends to expand more towards flood-prone areas ~~We also find that urban will tend to expand to areas vulnerable to floods~~ under the restriction of ecological environment protection. The increasing flood risk information determined by ~~the coupling~~ model simulations helps to understand the spatial distribution of future flood-prone urban areas and promote the re-formulation of urban planning in high-risk locations.

## 1 Introduction

Climate change and urbanization are the global challenges for the 21<sup>st</sup> century ( Ramaswami et al., 2016; Pecl et al., 2017). Floods have been key threats for many cities around the world driven by global climate change (Hallegatte et al., 2013;

31 IPCC, 2014; Fang et al., 2020). Currently, more than 600 million people worldwide live in ~~the~~ coastal cities that are less than  
32 10 m above sea level (United Nations, 2017). ~~The United Nations reports that the global population will increase by 29%~~  
33 ~~(7.6 billion) between 2017 and 2050 especially in some coastal countries (United Nations, 2017b), which means that~~  
34 ~~population of coastal cities will become increasingly concentrated in the future and impervious surfaces will become more~~  
35 ~~numerous~~ The United Nations reports that the global population living in cities is projected to reach 6.7 billion by 2050  
36 (United Nations, 2018), especially in low elevation coastal areas, the population density is expected to be twice the current  
37 population density (Van Coppenolle and Temmerman, 2019), which means that the population of coastal cities will become  
38 increasingly concentrated in the future and impervious surfaces will become more numerous (Chen et al., 2020; He et al.,  
39 2021). On the other hand, the National Oceanic and Atmospheric Administration (NOAA) report suggests that global mean  
40 sea level will rise around 0.2 m to 2.0 m by 2100 under a continuing global warming trend (Parris et al., 2012). Additionally,  
41 properties and populations in many coastal areas will suffer more severely in the future if the effects of land subsidence are  
42 taken into account (Vousdoukas et al., 2018).

43 However, high uncertainty in flood risk and urban growth leads to a lack of capacity of cities to respond to the flooding  
44 arising from future climate change (Du et al., 2015; Tessler et al., 2015; Fang et al., 2021). Therefore, there is an urgent need  
45 for specialist knowledge and techniques to address the conflict between urbanization and flood risk (-Wang et al., 2015; Lai  
46 et al., 2016; Bouwer, 2018; Haynes et al., 2018). ~~For example, flood risk studies focus mainly on the current urban scenarios~~  
47 ~~for disaster risk assessment (Bisht et al., 2016; Zhou et al., 2019); and partly consider future land use changes, but urban~~  
48 ~~growth scenarios are mainly limited to original typologies (business as usual development) growth scenarios for study~~  
49 ~~(Huong and Pathirana, 2013; Muis et al., 2015), with less consideration of environmental factors and urban growth scenarios~~  
50 ~~under planning constraints (Lin et al., 2020; Long and Wu, 2016); thus, the lack of knowledge of future urban development~~  
51 ~~scenarios leads to a lack of awareness of the consequences of future flooding~~ Studies on urban flood risk assessment are  
52 more likely to simulate flood risk using different climate change scenarios or integrating different flood sources (Huong and  
53 Pathirana, 2013; Muis et al., 2015; Dullo et al., 2021). For example, Zhou et al. examine the impact of urban flood volumes  
54 and associated risks under RCP2.6 and RCP8.5 scenarios (Zhou et al., 2019). Parodi et al. integrate the compound flood  
55 scenarios such as wave height, storm surge, and extreme sea level due to sea level rise to assess coastal flood risk (Parodi et  
56 al., 2020). However, ignoring the uncertainty of urban growth in urban flood risk assessment reduces the validity of the  
57 assessment (Gori et al., 2019), and hence an increased understanding of possible urban growth scenarios is needed, otherwise  
58 there is a lack of understanding of the consequences of future flooding (-Zhao et al., 2017; Kim and Newman, 2020).  
59 Although there are some studies that have quantified future growth scenarios for urbanization (-Nithila Devi et al., 2019; Lin  
60 et al., 2020), these studies have not considered the impact of existing planned policies that are designed to mitigate the  
61 impact of new development. On the other hand In addition, the failure to integrate with broader climate change-related  
62 scenarios and possible extreme-case flood risks has led to underinvestment in climate adaptation actions by governments that  
63 do not well address the spatial consequences of future floods (Reckien et al., 2018; Berke et al., 2019). Thus, there is an

64 urgent need to adopt a more comprehensive approach ~~that consider~~to assess the complexity of multiple possible scenarios of  
65 urbanization and dynamic flood risk in an integrated manner.

66 This paper uses the coupling of the future land use simulation model (FLUS) and the 2D floodplain inundation model  
67 (LISFLOOD-FP) to explore the possible interaction between different urbanization development scenarios and climate  
68 change scenarios. The FLUS model improves the simulation accuracy of the model by combining artificial neural network  
69 (ANN) and Cellular automata (CA) model to simulate nonlinear land use changes while considering parameters related to  
70 environment, society, climate change, etc. (Liu et al., 2017; Zhai et al., 2020). The LISFLOOD-FP model has become a  
71 mature hydrodynamic model that can predict potential flood events in near real-time and are widely used in engineering  
72 applications (-Wing et al., 2019; Sosa et al., 2020). The coastal metropolitan Area of Shanghai in the Yangtze River Delta in  
73 China, one of the fastest urbanizing cities in the world, is used as a case study.

74 The paper asks, how ~~can combining~~ different urban growth scenarios combined with climate change scenario analysis may  
75 help to inform preparedness for flood risks from climate change in urban flood risk assessments? To answer this question,  
76 we first assume some future simulation scenario by considering the factors that influence urban growth and lead to flood  
77 risk, we first consider how urban grow under different environmental and planning factors in the future. Secondly, we  
78 coupled urban growth and flood risk scenarios and compared them using climate change scenarios from two representative  
79 concentrated pathways (RCP 2.6 and 8.5) proposed by the Intergovernmental Panel on Climate Change (IPCC). Finally, we  
80 assessed the risk of flooding in different urban development scenarios. The research illustrates the importance of assessing  
81 the performance of different future urban development scenarios in response to climate change, and the simulation study of  
82 urban risks will prove to decision-makers that incorporating disaster prevention measures into urban development plans will  
83 help to reduce disaster losses and improve the ability of urban systems to respond to floods.

84 The rest of paper is organized as follows: section 2 describes the characteristics of the study area and presents the data used  
85 in this paper; followed by a description of the methodology for integrating future land use change models and hydrodynamic  
86 models in Section 3. The results and discussion in Section 4 and Section 5. We divided the discussion section into two parts,  
87 on the one hand discussing the sources of uncertainty in the study, and the other part discussing adaptation policies for urban  
88 flood risk in the context of climate change. The conclusion of the study is described in Section 6.

## 89 2 Study area and datasets

### 90 2.1 Study area

91 As the alluvial plain of the Yangtze River Delta, Shanghai is located on the coast of the East China Sea between 30°40'–  
92 31°53'N and 120°52'–122°12'E, which borders the provinces of Jiangsu and Zhejiang to the ~~west~~West (Fig. 1). It's a typical  
93 middle latitude transition belt, marine land transitional zone and also a typical estuarine and coastal city with a fragile  
94 ecological environment. The land area of Shanghai is about 6340.50 km<sup>2</sup>, accounting for 0.06 % of the total area of China,  
95 and has 213 km of coastlines. The Shanghai metropolitan area has undergone rapid urban expansion in the past decades and

has become one of the largest urban areas in the world in both size and population (Sun et al., 2020). However, Shanghai's topography is low, with an average elevation of 4 m above sea level, and there is no natural barrier against storm surges. In 1905, one of the deadliest storm surges occurred in Shanghai, killing more than 29,000 people. Two years later, Typhoon Winnie made landfall in Shanghai, flooded more than 5,000 households (Du et al., 2020). Additionally, due to land subsidence and the increasing frequency and intensity of storm surges, Shanghai will become one of the most sensitive regions due to the global climate change.

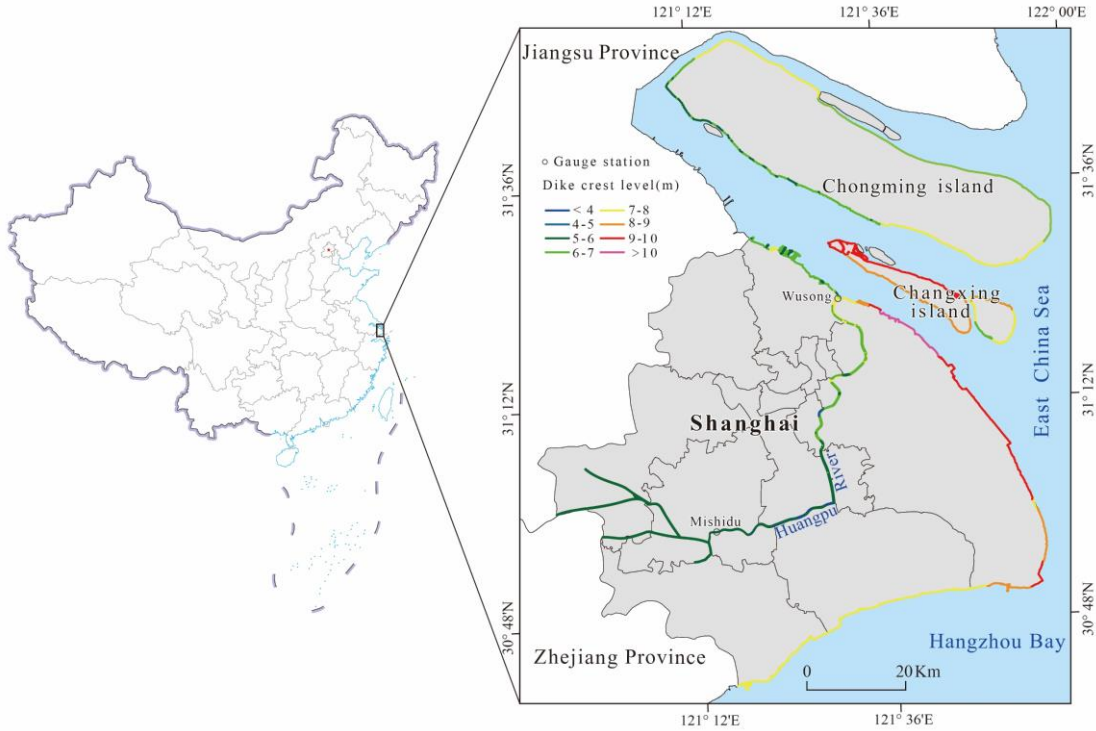


**Figure 1: Location map of the study area. The main inland rivers in Shanghai flow into the East China Sea through the Huangpu River. The line with coloured vectors in the figure indicates the different dike crest level in Shanghai.**

## 2.2 Data

The research used three main categories of data, including basic data, scenarios constraints data and flood simulation data (Table 1). The basic data include land use, topography, traffic network, traffic site, socio-economic data. The land use data with a resolution of 100 m×100 m from the Resource and Environmental Science and Data Center of the Chinese Academy of Sciences is currently the most accurate land use remote sensing monitoring data product in China (Liu et al., 2014). The data for 2005 and 2010 were derived from Landsat-TM/ETM remote sensing image data respectively, and the data for 2015 were interpreted using Landsat 8 remote sensing image. After the data was corrected and manually visually interpreted, the comprehensive evaluation accuracy of the interpretation accuracy of the first-class types of cultivated land, woodland,

grassland, water area, urban land, and unused land reached more than 94.30\_%, and the discrimination accuracy rate on the map patches reached 98.70\_% (Xu et al., 2017). Within the allowable error range, it can be used as the basic data for analyzing land use changes.

Topography factors (DEM, slope), traffic network factors (distance to railway, highway, subway, and main roads), traffic site factors (distance to the city center, train station, and airports) and socio-economic factors (population, GDP), etc. as well as planning constraints, were determined to be spatial influence factors of the flood risk assessment of the Shanghai area. The Advanced Spaceborne Thermal Emission and Reflection Radiometer (ASTER) digital elevation model (DEM), which has 30-meter resolution, served as the basis data for terrain heights and slopes. ASTER-DEM has been shown to be the most stable data performer among six types of open access DEM products (SRTM, ASTER-DEM, AW3D, MERIT, NASADEM and CoastalDEM) for flood inundation simulations with different return periods (Xu et al., 2021). Traffic network and site were collected from open-source data retrieved from OpenStreetMap (OSM) and POI data were extracted from Tencent Map. Euclidean distance was calculated for all vector data. The data of population and gross domestic product (GDP), were provided by the Resource and Environmental Science and Data Center of the Chinese Academy of Sciences (Xu, 2017a, 2017b), and their time span was consistent with the land use data. According to the simulation forecast demand, all materials were converted into 100 × 100 m grid by resampling. The spatial limiting factors were the basic ecological control line, permanent basic cropland and cultural protection control line as outlined in the 2017–2035 Shanghai City Master Plan. All the impact factor data were normalized, and the range of the value is between 0 and 1 to subsequent data mining.

The storm surge data comes from the Global Tide and Surge Reanalysis (GTSR) dataset, which has been ~~validation~~-validated to have good accuracy (Muis et al., 2016). In addition, man-made flood defenses have been considered to reasonably evaluate the inundation impact of the flooding. The coastal flood protection data was obtained from the historical archival of the Shanghai Water Authority for Shanghai (Yin et al., 2020). All data sources are listed in in the table below.

**Table 24. Data required and sources. The list details the resolution and sources of the data in the study.**

Category	Data Type	Resolution	Source
Basic data	Land use	100 m × 100m	Resource and Environmental Science and Data Center ( <a href="http://www.resdc.cn">http://www.resdc.cn</a> )
	Topography	Vector line	ASTER GDEM ( <a href="https://earthexplorer.usgs.gov/">https://earthexplorer.usgs.gov/</a> )
	Traffic network	Vector line	OpenStreetMap ( <a href="https://www.openstreetmap.org">https://www.openstreetmap.org</a> )
	Traffic site	Vector point	Tencent Map ( <a href="https://map.qq.com/">https://map.qq.com/</a> )
	Social economy	1 km × 1 km	Resource and Environmental Science and Data Center
<u>Scenarios constraints</u>	Ecological control line	Vector line	<u>《2017-2035 Shanghai City Master</u>

	Permanent basic cropland control line	Vector line	Plan»
	Cultural protection control line	Vector line	
Flood data	Floodwalls	Vector line	Shanghai Water Authority ( <a href="http://swj.sh.gov.cn/">http://swj.sh.gov.cn/</a> )
	Storm surge	Vector line	GTSR

135 **3 Methodology**

136 The presented approach for relative sea level rise scenario flood risk assessment is the integration of the FLUS model,  
137 LISFLOOD-FP model, and Markov chain model. In the framework, the FLUS model and Markov chain model are designed  
138 to stimulate complex~~ity~~ land-use change processes in three different scenarios through 2030 to 2050, which include Business  
139 as usual (BU), Growth as planned (GP), Growth as eco-constraints (GE) scenarios. A Markov chain model is used to predict  
140 land-use demand in 2030 and 2050. ~~combine~~combining planning policy factors, which is one of the crucial data inputs in the  
141 FLUS model. Next, the LISFLOOD-FP two-dimensional flood model is used to explore the potential flooding areas under  
142 the RCP 2.6 and 8.5 scenarios in 2030 and 2050, to avoid the overestimation of the submerged range based on the GIS-based  
143 elevation area method. This model also considers the compound influence of sea-level rise, storm surge, and land  
144 ~~subsidence~~, ~~Finally~~subsidence. ~~Finally~~, via ArcGIS spatial comprehensive analysis, the flooding of different land types is  
145 calculated employing different flooding scenarios. The overall flow chart of research is illustrated in Fig. 2.

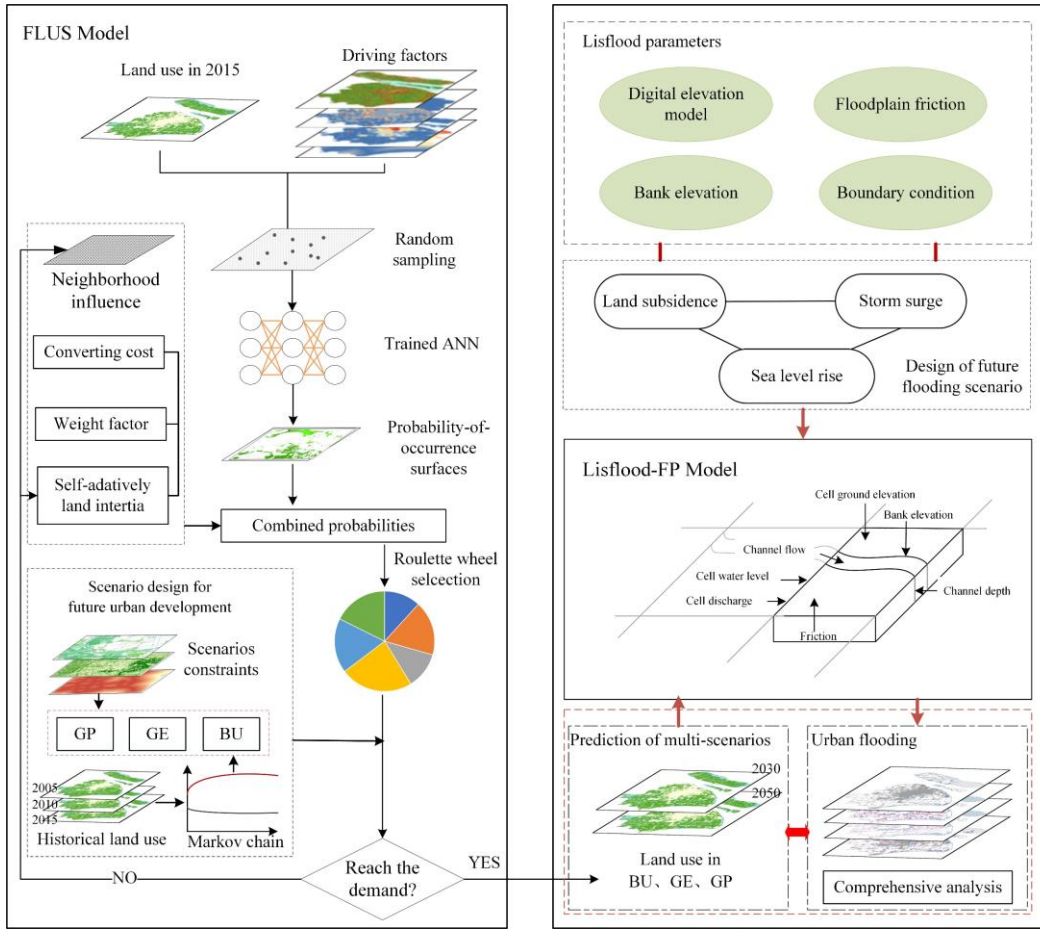


**Figure 2: The overall flow chart of research.**

### 3.1 Markov chain model

Markov chain model refers to the random transition process of state from one state to another, and its future state is only related to the state at previous moment. In the study of land use change, the type of land use at a certain moment is only related to the type of land use at the previous moment. Therefore, land-use change is a typical Markov process and has widely used in the prediction of land-use changes (Zhou et al., 2020). We predicted future land use by Eq. (1):

$$S_{(t+1)} = P_{i,j} \times S_t \quad (1)$$

where  $S_t$  and  $S_{t+1}$  represent the land use at times  $t$  and  $t+1$ , and  $P_{i,j}$  is a state transition matrix that land-use type  $i$  is converted to land-use type  $j$ . This model has a good predictive effect on the process state (Gounaridis et al., 2019). Therefore, we use the Markov chain to calculate the probability of the conversion of various land types, and then predict the number of future land changes.



### 158 3.2 The FLUS land use simulation model

159 The FLUS model is an upgraded version of a cellular automata model (Liu et al., 2017)~~—~~ which can solve the complex land  
160 use simulation problems by self-adaptive inertia and competition mechanism. The FLUS shows the highest current  
161 performances than other simulation models such as CLEU-S, SLEUTH, and LTM and has been applied to land use change  
162 simulation research at different scales and for different purposes (Liang et al., 2018; Lin et al., 2020).

163 As the most important scheme to manage the space of the urban area, an urban land use plan can reflect the general  
164 arrangement of land use in the future (Xu and Yang, 2019). In this research, three categories of urban growth scenarios are  
165 simulated through the FLUS model. The similarity of the three scenarios is that they use factors that affect urban  
166 development and changes, such as population, GDP, traffic, and slope, as the main spatial driving factors. The difference ~~is~~  
167 are as follows:

168 (i) Business as usual (BU): BU is natural growth without development laws and regulations. Its development is based on the  
169 premise of the current urban development patterns. Therefore, the land demand predicted by Markov is used as the constraint  
170 condition for the iteration of CA model in the subsequent application of the scenario.

171 (ii) Growth as planned (GP): Under the GP scenario, the urban growth projection that closely link to the master plan for  
172 Shanghai in terms of quantity, reflecting how the city government prefer to develop. The master plan requires that the total  
173 area of planned urban construction land does not exceed 3,200 km<sup>2</sup> in 2035. We choose an urban area of 2768 km<sup>2</sup> in 2030  
174 and 3200 km<sup>2</sup> in 2050 as the constraints under the GP scenario. The reason is that the Markov chain model projections result  
175 in an urban area is 2768 km<sup>2</sup> in 2030 and 3270 km<sup>2</sup> in 2050, and the total urban construction land area in 2035 of the  
176 Shanghai Master Plan does not exceed 3200 km<sup>2</sup>.As the condition for the model iteration to stop, we estimated the urban  
177 area to be 2,768 km<sup>2</sup> in 2030 and 3,200 km<sup>2</sup> in 2050 combined with urban master plan.

178 (iii) Growth as eco-constraints (GE): The GE scenario is an eco-environmental protection scenario which development is  
179 limited by the ecological environment protection. Combined with Shanghai's ecological and environmental protection  
180 requirements and the distribution of permanent basic farmland, sensitive areas restricted for development are identified at the  
181 scenario, and we also establish a cultural protection control line for strengthening historical and cultural protection. In  
182 addition, the number of areas of future urban growth in the GE scenario also combines the requirements given in the urban  
183 master plan to enhance the reality of the scenario.

184 Therefore, the FLUS model is used to simulate future urban growth ~~combines-combining~~ various scenarios. First, the driving  
185 factors and land-use data ~~is-are~~ trained by an ANN model to obtain a probability-of-occurrence map, and then incorporate  
186 with the self-adaptive land inertial, conversion cost, and neighborhood competition among the different land use types to  
187 estimate the combined probability for each grid. Next, combining the number of various types of land predicted by the  
188 Markov Chain model and considering the constraints of each scenario to predicted urban growth in 2030 and 2050. To better  
189 validate the model before predicting ~~for~~ future change, we compared the output ~~to-with~~ the actual land use 2015. Note that



190 the number of iterations in each scenario is set to 5000, which is much higher than the default value to show higher  
191 prediction accuracy.

### 192 3.3 The LISFLOOD-FP flood inundation model

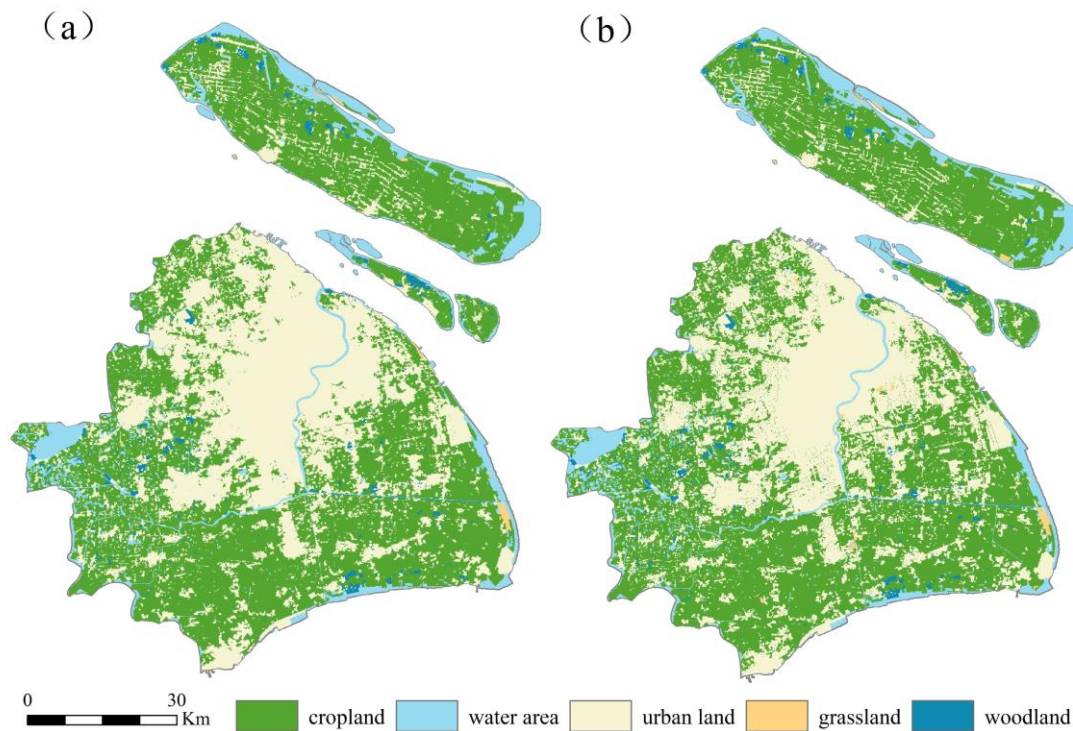
193 LISFLOOD-FP is a 2D hydraulic model based on a raster grid (Bates et al., 2010), which can efficiently simulate the  
194 dynamic propagation of flood waves over fluvial and estuarine floodplains and show real-time changes in water depth of  
195 complex terrain. LISFLOOD-FP model solves the Saint-Venant equations at very low computational cost by omitting only  
196 the convective acceleration term over a structured grid using a highly efficient explicit finite difference scheme to produce a  
197 two-dimensional simulation of floodplain hydrodynamics (O’Loughlin et al., 2020). The model has been widely used in the  
198 applications of small-scale and large-scale urban waterlogging and flooding\_ (Hoch et al., 2019; Rajib et al., 2020; Zhao et  
199 al., 2020).

200 In the present study, the LISFLOOD-FP model is used to simulate storm surge floods along the coast of Shanghai and floods  
201 along the Huangpu River. The effectiveness of the model in the study area has been verified by another article of our group  
202 members and shows good simulation results(Xu et al., 2021). In the boundary control of model, hydrological stations and  
203 global storm surge data are respectively employed as the input of the scenario design. However, Shanghai Geological  
204 Environmental Bulletin and land subsidence control plan show that land subsidence has a significant contribution to the  
205 flood hazards in Shanghai (Xian et al., 2018).~~With reference to the research of Yin et al (Yin et al., 2013), Land subsidence~~  
206 ~~in Shanghai is mainly caused by tectonic subsidence and compaction of sediments due to geological structure conditions and~~  
207 ~~human activities. With reference to the long-term tectonic subsidence monitoring data of the very long baseline~~  
208 ~~interferometer (VLBI) in the Sheshan bedrock and the land subsidence analysis rules of Yin et al. (Yin et al., 2013).~~  
209 ~~therefore, the total land subsidence is predicted to be 0.12 m and 0.24 m by 2030 and 2050, respectively. However, due to~~  
210 ~~the uncertainty of future anthropogenic activities and spatial distribution, there could be large variations in the the values of~~  
211 ~~land subsidence in 2030 and 2050 are selected to be 0.12 m and 0.24 m, respectively. This projection. This~~ study also  
212 combines the storyline of future scenarios of the IPCC, namely the Representative Concentration Pathway (RCP) scenarios,  
213 and selects conservative (RCP2.6) and largest magnitude (RCP8.5) climate-change scenarios, ~~which-with~~ values from Kopp  
214 et al (Kopp et al., 2017). For the simulation of the Huangpu River flood, we conducted experiments for a 50-year return  
215 period under the RCP2.6 scenario and a 100-year return period under the RCP8.5 scenario respectively during 2030 to 2050.  
216 For the 2030 and 2050, both Huangpu River and the coastal floods are ~~followed-to~~following the RCP2.6 and RCP8.5  
217 scenarios. Finally, we combine land subsidence and the RCP data to control the flood inundation simulation.

218 **4 Results**

219 **4.1 Model validity**

220 Model verification is the prerequisite for model operation, and the operation can only be carried out after confirming the  
221 model ~~that is considered to be~~ valid. The applicability of the proposed model was tested by simulating land use/cover changes  
222 (LUCCs) in 2015 at Shanghai. The spatial simulation result shows that the simulated result and the actual land use have a  
223 high consistency (Fig. 3). We compared the actual land use and the simulated result pixel by pixel in our study and found the  
224 overall accuracy (OA) was 93.20 %, the kappa coefficient (kappa) was 0.89. The discrepancy of the actual land use and  
225 simulated result is likely due to the neighborhood interaction in the CA model, in which grid cells in more urbanized  
226 neighborhoods have a higher probability to convert to urban, whereas the grid cells are less likely to change to urban in less  
227 urbanized neighborhoods. Overall, the measured model accuracy outputs ~~are measured shows showed~~ an acceptable or good  
228 level of prediction, therefore the model is suitable for predicting changes in land use of the Shanghai area.



229 **Figure 3: Comparing the simulation results of Shanghai urban expansion with the actual situation, (a) simulation result in 2015;**  
230 **(b) actual land use in 2015.**

232 **4.2 Future land use changes**

233 Based on the conditions under three different development scenarios, we predicted the development of future urban land use  
234 change in 2030 and 2050. The prediction result shows different development patterns for each scenario (Fig. 4). Future urban  
235 growth under the BU scenario is primarily located in northwestern with some development in the central regions, and under  
236 the GP scenario the urban growth involves evenly distributed development. Urban growth in the GE scenario, however,  
237 Chongming Island regions have seen more urban growth, and the downtown area is not fully occupied by urban expansion  
238 due to restrictions.

239 Due to the impact of infrastructure construction, distance to the city center, and policy restrictions, Shanghai's overall urban  
240 expansion model shows a center-peripheral expansion. The built-up land areas in 2030 and 2050 are respectively projected~~ed~~ to  
241 increase by about 6 % and 13 % as compared~~d~~ to 2015, the most significant reduction is found for cultivated land and  
242 woodland. Specifically, the built-up land areas in 2030 are respectively projected~~ed~~ to increase by 427.32 km<sup>2</sup>, 428.27 km<sup>2</sup> and  
243 429.12 km<sup>2</sup> at BU, GP and GE scenarios, the built-up land areas in 2050 are respectively projected~~ed~~ to increase by 926.38  
244 km<sup>2</sup>, 857.63 km<sup>2</sup> and 751.47 km<sup>2</sup> at BU, GP and GE scenarios. The most significant reduction is found for cropland, which is  
245 predicting in 2050 to decrease by 876.97 km<sup>2</sup>, 857.63 km<sup>2</sup> and 723.59 km<sup>2</sup> as compared to 2015 in BU, GP and GE  
246 scenarios. The southwestern region is not suitable for large-scale urban development, ~~due to~~since large amounts of farmland  
247 in the region are listed as ecological protection areas, so the slow growth of these areas is not expected. The simulation maps  
248 show, as expected, land use changes under different planning scenarios, especially the urban sprawl trend at the GE scenario,  
249 creating new development areas in suburbs. To sum up, the urban expansion trajectory under BU, GP and GE shows  
250 significant differences, and these changes mainly at the expense of the cropland.

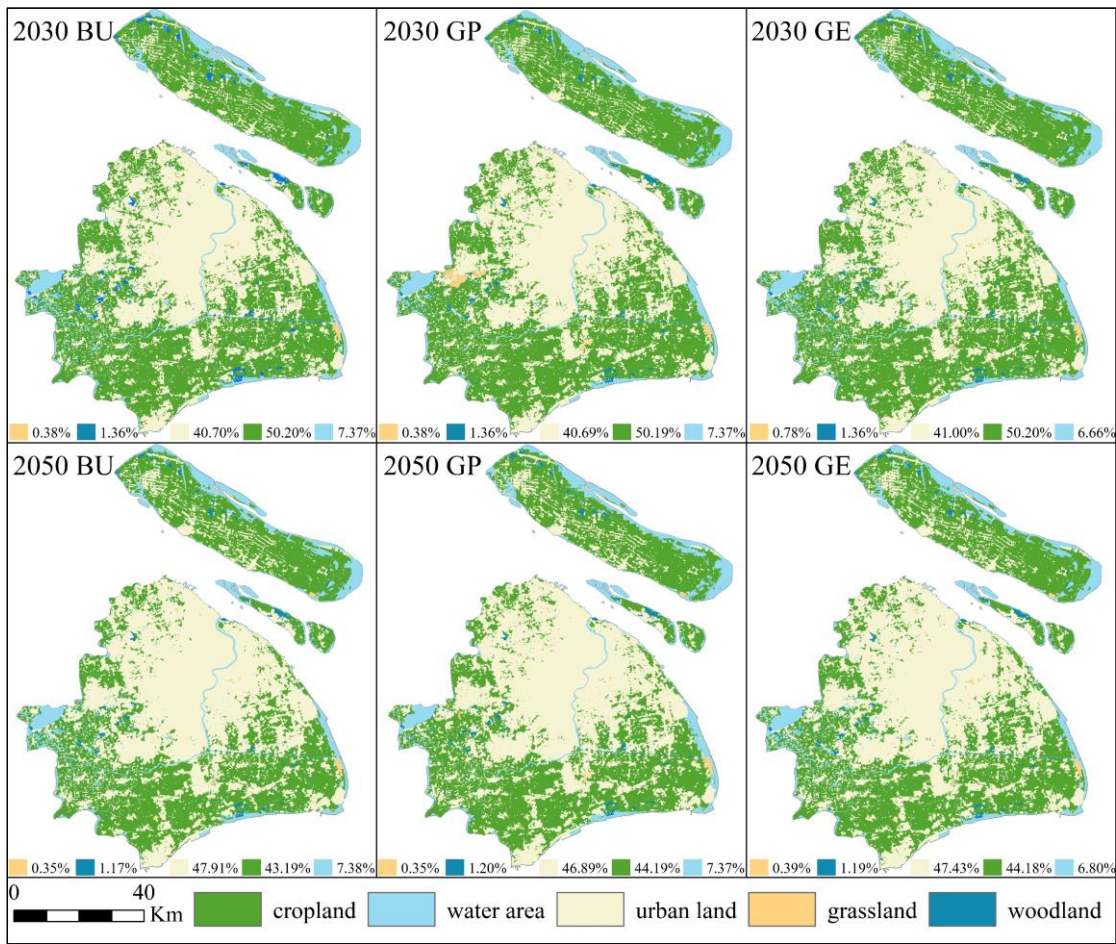


**Figure 4: Simulation results of different scenarios in 2030 (top) and 2050 (bottom). Each image shows the spatial distribution and the proportion of area of different land use types in the simulated scenario.**

### 4.3 Changing flood hazard in the future

The LISFLOOD-FP model is used to simulate the flood evolution process under RCP2.6 and RCP8.5 scenarios (the inundation results are plotted in Supplementary Figure 1), and then the submerged depth and area under different scenarios are statistically analyzed to explore the future flood risk under different RCP scenarios. First, the maximum water depth risk of the submerged area is counted, and the submerged area is divided into four depth levels: the submerged water depth is less than 0.5 m as shallow water area, water depth is 0.5-1 m as medium water area, the water depth is 1-2 m as deep water area, and submerged water depth is above 2 m as the extremely deep area. The area and proportion of each water depth level are calculated.

By comparing the scenarios in RCP2.6 and RCP8.5, it is evident that the submerged area is increasing ~~trends~~ with time (Table 2). The total flooded area increased by 162.43 km<sup>2</sup> and 189.44 km<sup>2</sup> under RCP2.6 and RCP8.5 scenarios from 2030 to

2050, respectively. Additionally, the depth of submergence and the extent of submergence will gradually increase as the floodwater spreads. Taking the area with submergence depth above 2 m as an example, under RCP2.6 scenario the area with submergence is 353.69 km<sup>2</sup> and 401.57 km<sup>2</sup> respectively in 2030 and 2050, and under RCP8.5 scenario the area with submergence is 356.28 km<sup>2</sup> and 418.36 km<sup>2</sup> respectively in 2030 and 2050. It shows that Shanghai will still face great flood risk under these two scenarios.

**Table 2. Statistics of flood water depth.**

Category	<0.5 m		0.5-1 m		1-2 m		>2 m		Total /km <sup>2</sup>
	Area/ km <sup>2</sup>	Ratio/ %	Area/ km <sup>2</sup>	Ratio/ %	Area/ km <sup>2</sup>	Ratio/ %	Area/ km <sup>2</sup>	Ratio/ %	
2030 RCP2.6	138.61	14.54	164.07	17.21	296.98	31.15	353.69	37.10	953.35
2030 RCP8.5	137.13	14.23	169.76	17.61	300.82	31.21	356.28	36.96	963.99
2050 RCP2.6	125.04	11.21	229.81	20.60	359.36	32.21	401.57	35.99	1115.78
2050 RCP8.5	141.72	12.29	219.58	19.04	373.77	32.41	418.36	36.27	1153.43

#### 4.4 Future changes in urban flood risk

The flood risk of the urban [area](#) is calculated by overlapping existing urban and projected future urban scenarios with future flood risk zones. First, in the existing urban exposure to future flood risk scenarios (the upper left in Fig. 5), more urban areas will be vulnerable to flood risk in the context of global climate change. [The four pie charts for the EU scenarios represent the proportion of the existing urban area affected by the future flood risk scenario.](#) Under the RCP 2.6 scenario, 4.68 % and 5.96 % of the total existing urban areas in 2030 and 2050 would be susceptible to flood risk, respectively. In the 2030 and 2050 of the RCP8.5 scenarios the area of existing urban land which would be vulnerable to future flood risks are 110.27 km<sup>2</sup> and 146.23 km<sup>2</sup>, respectively. Many urban areas will be flooded under sea level rise caused by climate change even when protected by levees, and more than 5 % of urban areas in Shanghai are still in the floodplain [\(Fig. 5\)](#).



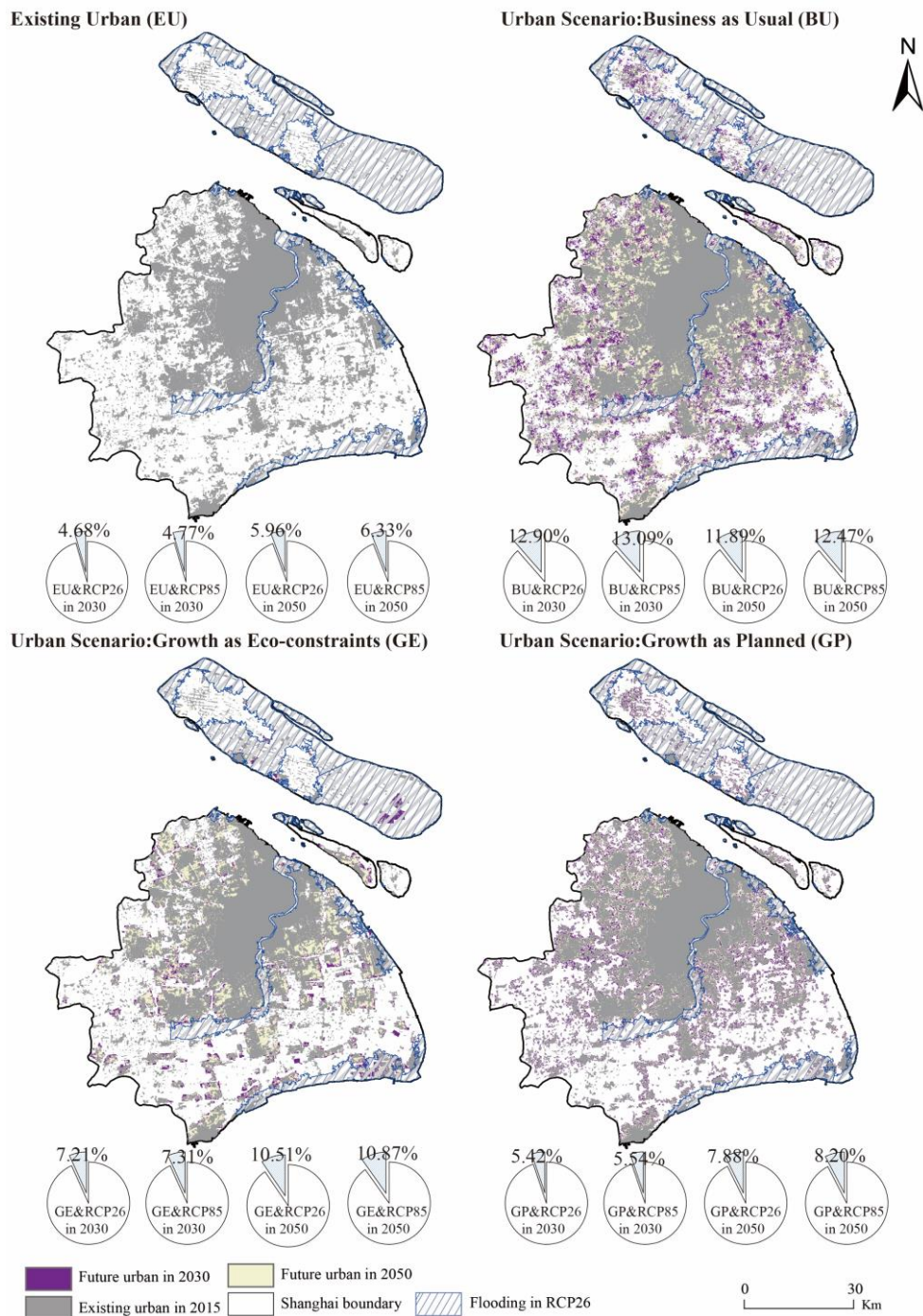


**Figure 5: Flood exposure of existing urban and future urban growth scenarios. The four pie charts for the BU, GE, and GP scenarios represent the proportion of new growth-grown urban area exposed to flooding under the 2030\_RCP2.6, 2030\_RCP8.5, 2050\_RCP2.6, and 2050\_RCP8.5 scenarios, respectively. The four pie charts for the EU scenarios represent the proportion of the existing urban area affected by the future flood risk scenario.**

284 Future urban development would occur in the flood zone, with ~~the a~~ rapid expansion of the urban area. Fig. 5 also shows the  
 285 comprehensive analysis results of the three urban growth scenarios under different climate change scenarios. Under the  
 286 RCP2.6 scenario, new growth in urban land area affected by flooding in 2030 are respectively 55.11 km<sup>2</sup>, 23.22 km<sup>2</sup>, and  
 287 30.92 km<sup>2</sup> at BU, GP and GE scenarios. Under the RCP8.5 scenario, future more urban growth areas would be affected by  
 288 the flooding, which will ~~be-reached~~ 115.53 km<sup>2</sup>12.47 %, 70.36 km<sup>2</sup>10.87 %, and 81.71 km<sup>2</sup>8.20 % at BU, GP and GE  
 289 scenarios in 2050, respectively. In general, the higher the sea level rises, the greater the risk of flooding in future urban areas.  
 290 Small changes in sea level rise will affect a large amount of land, ~~due to~~since the average altitude of Shanghai is only around  
 291 4 m.

292 **Table 3. ~~Inundate~~ Inundation of each land use type under different scenarios. The inundated areas of different land use types,**  
 293 **including cropland, woodland, grassland and urban land, were calculated for each scenario, where <sup>a</sup> indicates new ~~growth~~ grown**  
 294 **areas of the urban class affected by flooding.**

Time	Category	Urban scenario	Inundated areas (km <sup>2</sup> )			
			Cropland	Woodland	Grassland	Urban land <sup>a</sup>
2030	RCP2.6	BU	595.05	10.05	5.60	55.11
		GE	618.95	12.12	5.84	30.92
		GP	597.71	12.40	5.91	23.22
	RCP8.5	BU	602.38	10.23	5.67	55.92
		GE	625.97	12.29	5.91	31.23
		GP	604.32	12.59	5.98	23.72
2050	RCP2.6	BU	662.64	13.56	5.25	110.19
		GE	677.59	16.74	5.95	78.95
		GP	651.24	15.66	5.46	67.55
	RCP8.5	BU	683.56	15.06	5.70	115.53
		GE	698.98	18.05	6.40	81.71
		GP	672.30	16.85	5.91	70.36

295  
 296 The research found that the cultivated land is the most affected land type by flooding relative to urban areas, woodland and  
 297 grassland ~~The research found that the cultivated land is most affected by flooding~~ (Table 3), ~~and urban areas and woodland~~  
 298 ~~are the second most affected~~. Under the GE scenario, the flooded area of cultivated land is 618.95 km<sup>2</sup> and 625.97 km<sup>2</sup> at the  
 299 RCP2.6 and RCP8.5 in 2030, and 677.59 km<sup>2</sup> and 698.98 km<sup>2</sup> at the RCP2.6 and RCP8.5 in 2050. Further, the exposure of



300 various types of land is increasing with time, but urban land and cropland will be the most impacted land types in the future.  
301 Comparing the three scenarios we can find that the urban development area under the planning scenario is less affected by  
302 flooding, as compared to the business-as-usual development scenario. Comparing the inundation of the two planning  
303 scenarios (GE and GP), it also reflects the decision-makers' trade-off between economic development and ecological  
304 protection. The inundation area of the urban land under the GP scenario is less than that of the GE, which means that under  
305 the planning constraint of protecting ecological and cultural areas, urban built-up areas will develop on low-protection areas,  
306 which are more vulnerable to flooding. In conclusion, from reducing the risk of future flooding in urban areas, GE scenario  
307 shows to be better than BU scenario, but worse than GP scenario.

## 308 5 Discussions

### 309 5.1 Source of uncertainties

310 There are some limitations in our study, which is what we need to improve in the future. First, there is still more room to  
311 improve the accuracy of model prediction. In this study, the performance of the FLUS model is tested by kappa and OA  
312 measures, which shows a good range of prediction accuracy. In addition, this study proves that 16 driving factors contribute  
313 to the simulation and prediction of urban growth in Shanghai. The relationship between human and natural driving factors  
314 and land use change can be effectively integrated through the FLUS model embedded with an ANN, to obtain more realistic  
315 simulation results. However, if more influential drivers and the latest land cover are employed, the prediction would be  
316 having higher accuracy. Second, future flood risks in coastal areas are also ~~are~~ not fully reflected through ~~using the use~~ of  
317 hydrodynamic models, although it shows higher accuracy than the elevation area submergence method. On the one hand, this  
318 study is based on the modeling results of DEM data, which may overestimate or underestimate the simulation effect due to  
319 the error of DEM data. On the other hand, extreme storm surge and land subsidence data are combined to enhance the  
320 reliability of the extreme flood forecast in this study. However, the change of the impervious surface that affects hydrology  
321 is not ~~be yet~~ considered in this study. When other land uses are converted to urban land uses, the risk of flooding will also  
322 greatly increase due to changes the of impervious surfaces. Therefore, it is necessary to dynamically adjust relevant factors  
323 affecting flood peak flows and risk in future forecasts to enhance the accuracy of prediction.

324 In the context of global climate change, extreme weather in the future may become more and more serious, so it is necessary  
325 to dynamically combine climate scenarios to develop more accurate flood risk delineation methods to guide urban planning  
326 in the future, and rely on new technology and equipment to provide data support. For example, unmanned aviation vehicles  
327 (UAVs) are deployed around the coastline to generate real-time information about weather conditions and sea-level changes  
328 (Cochrane et al., 2017). These tools will act as a complement to existing information and early warning systems, which also  
329 can provide guidance for coastal flood risk management and urban planning in the future. Overall, although uncertainty  
330 cannot be avoided when assessing coastal flood risk, the deviation of the proposed model output is within an acceptable  
331 range, which ensures the accuracy of coastal flood risk assessments.

## 332 5.2 Recommendations on strategies and policies for urban adaptation to flooding

333 In the twenty-first century, adapting to climate change and coastal flooding is a critical challenge for coastal cities. Human  
334 response to the impacts of flooding largely depends on the allocation of urban facilities and managers' planning for future  
335 urban development (Hunt and Watkiss, 2011). Shanghai is considered one of the most protected Chinese cities in terms of  
336 flood protection, yet it's the EAD/GDP (the Expected Annual Disruption, EAD), that is the direct damage to buildings and  
337 vehicles) ratio, which is as much as five times than in New York (Aerts et al., 2014). Therefore, there is an urgent need to  
338 adopt flood risk adaptation strategies in Shanghai.

339 We conducted a set of comparative experiments to analyze the coastal flood damage in Shanghai with and without flood  
340 walls (hard adaptation strategies). Our analysis considered the important effects of land subsidence and SLR-sea level rise on  
341 flood risk. We found that the current flood protection wall can reduce the flood losses due to climate change to a relatively  
342 low level (Supplementary Figure 2). In comparison, the flood protection wall constructed for the current conditions would  
343 reduce the flooded area under the RCP8.5 scenario by about 35\_% and 36\_% in 2030 and 2050, respectively. ~~This result~~  
344 ~~shows that the current hard protection strategy can reduce the flood risk to a low level, but the residual flood risk from using~~  
345 ~~the hard protection strategies still needs to be addressed. From the cases of advanced flood risk management countries such~~  
346 ~~as the Netherlands (Kabat et al., 2009; Song et al., 2018), an important success lesson for future flood protection design is to~~  
347 ~~leave enough space along coasts for wetland migration and leave space for nature. In other words, "soft strategies" such as~~  
348 ~~"working with rivers and nature" are considered in the flood protection measures. Therefore, it is necessary to learn from the~~  
349 ~~practical experience of advanced countries to strengthen the development and construction of coastal wetlands and tidal flat~~  
350 ~~ecosystems, and further reduce the residual risk through the adaptive regulation of coastal ecosystems and other soft~~  
351 ~~strategies. Furthermore, our results show that the area of future urban flood risk varies by scenario. Although the GE~~  
352 ~~scenario performs higher than the GP scenario in terms of flood inundation area, this does not mean that the GE scenario is~~  
353 ~~worse. From the cases of advanced flood risk management countries such as the Netherlands (Kabat et al., 2009; Song et al.,~~  
354 ~~2018), an important success lesson for future flood protection design is to leave enough space along coasts for wetland~~  
355 ~~migration and leave space for nature. In other words, "soft strategies" such as "working with rivers and nature" are~~  
356 ~~considered in the flood protection measures. Therefore, from this perspective the GE scenario may be a more likely future~~  
357 ~~development scenario among these three scenarios. Future, it is necessary to learn from the practical experience of advanced~~  
358 ~~countries to strengthen the development and construction of coastal wetlands and tidal flat ecosystems, and further reduce~~  
359 ~~the residual risk through the adaptive regulation of coastal ecosystems and other soft strategies.~~ In addition, the  
360 implementation of "soft strategies" can increase the value of ecosystem services, increase biodiversity and carbon  
361 sequestration, and improve social welfare (Du et al., 2020).

362 **6 Conclusion**

363 Scenario-based assessment has been found to be a powerful approach in numerous flood risk studies. This study combines an  
364 urban growth model with a two-dimensional flood inundation model to not only simulate urban development dynamics more  
365 accurately, but also to discard the shortcomings of the traditional elevation inundation method of overestimating inundation  
366 areas. We have also tested the resilience of Shanghai to future different climate scenarios with the current flood wall. The  
367 results of the study are beneficial to local planners and coastal managers in making decisions of future protected areas and  
368 developments.

369 This study employed three urban development scenarios and detected the relationships of urbanization and climate changes  
370 in 2030 and 2050. The results of the study show that urban growth under the three scenario models manifests significant  
371 differences in expansion trajectories, influenced by key factors such as infrastructure development and policy constraints.  
372 According to the predicted results of flood, new built-up areas are also potentially vulnerable areas of flood risk. New built-  
373 up areas under different scenarios show significant vulnerability and exposure risk under different climate scenarios, even  
374 with the support of flood bank and other hard structures. Additionally, the research provided significant insights into the  
375 range and spatial distribution of flood risk in future urban areas.

376 The current study is based on the multi scenario analysis of RCP global warming scenarios. In the future, the shared  
377 socioeconomic pathways (SSPs) can be combined to predict land use change, which make urban development scenarios ~~have~~  
378 more realistic choices. The results of this study estimate the future urban flood exposure areas, but this does not mean that all  
379 flood-vulnerable areas will be flooded, only that in these areas, the probability of each possible occurrence is greater.  
380 Therefore, proper preparations (such as definition restricted development zones) can reduce the damage risk of future flood  
381 and build more resilient cities.

382 **Author contributions**

383 Q. Sun and J. Fang designed the research; Q. Sun, K. Xu and X. Dang collected the data and carried out the experiments; Q.  
384 Sun wrote the draft; J. Fang, X. Dang, Y. Fang and M. Liu revised the manuscript; J. Fang, X. Li and M. Liu supervised and  
385 provided critical feedback. All authors contributed to the final version of the manuscript.

386 **Competing interests**

387 The authors declare that they have no conflict of interest.

388 **Funding source**

389 This work was supported by a grant from the National Natural Science Foundation of China (~~No.~~42001096, [41730646](#));  
390 Shanghai Sailing Program (19YF1413700); China Postdoctoral Science Foundation (~~No.~~2019M651429-); [East China](#)  
391 [Normal University Institute of Belt and Road & Global Development \(ECNU-BRGD-202106\)](#), and the National Key R&D  
392 [Program of China \(2017YFE0100700\)](#).

393 **References**

394 Aerts, J. C. J. H., Botzen, W. J. W., Emanuel, K., Lin, N., De Moel, H. and Michel-Kerjan, E. O.: Climate adaptation:  
395 Evaluating flood resilience strategies for coastal megacities, *Science* (80-. ), 344(6183), 473–475,  
396 doi:10.1126/science.1248222, 2014.

397 Bates, P. D., Horritt, M. S. and Fewtrell, T. J.: A simple inertial formulation of the shallow water equations for efficient two-  
398 dimensional flood inundation modelling, *J. Hydrol.*, 387(1–2), 33–45, doi:10.1016/j.jhydrol.2010.03.027, 2010.

399 Berke, P. R., Malecha, M. L., Yu, S., Lee, J. and Masterson, J. H.: Plan integration for resilience scorecard: evaluating  
400 networks of plans in six US coastal cities, *J. Environ. Plan. Manag.*, 62(5), 901–920,  
401 doi:10.1080/09640568.2018.1453354, 2019.

402 Bouwer, L. M.: Next-generation coastal risk models, *Nat. Clim. Chang.*, 8(9), 765–766, doi:10.1038/s41558-018-0262-2,  
403 2018.

404 Chen, G., Li, X., Liu, X., Chen, Y., Liang, X., Leng, J., Xu, X., Liao, W., Qiu, Y., Wu, Q. and Huang, K.: Global projections  
405 of future urban land expansion under shared socioeconomic pathways, *Nat. Commun.*, 11(1), 537, doi:10.1038/s41467-  
406 020-14386-x, 2020.

407 Cochrane, L., Cundill, G., Ludi, E., New, M., Nicholls, R. J., Wester, P., Cantin, B., Murali, K. S., Leone, M., Kituyi, E. and  
408 Landry, M. E.: A reflection on collaborative adaptation research in Africa and Asia, *Reg. Environ. Chang.*, 17(5), 1553–  
409 1561, doi:10.1007/s10113-017-1140-6, 2017.

410 Van Coppenolle, R. and Temmerman, S.: A global exploration of tidal wetland creation for nature-based flood risk  
411 mitigation in coastal cities, *Estuar. Coast. Shelf Sci.*, 226, 106262, doi:10.1016/j.ecss.2019.106262, 2019.

412 Du, S., Van Rompaey, A., Shi, P. and Wang, J.: A dual effect of urban expansion on flood risk in the Pearl River Delta  
413 (China) revealed by land-use scenarios and direct runoff simulation, *Nat. Hazards*, 77(1), 111–128,  
414 doi:10.1007/s11069-014-1583-8, 2015.

415 Du, S., Scussolini, P., Ward, P. J., Zhang, M., Wen, J., Wang, L., Koks, E., Diaz-Loaiza, A., Gao, J., Ke, Q. and Aerts, J. C.  
416 J. H.: Hard or soft flood adaptation? Advantages of a hybrid strategy for Shanghai, *Glob. Environ. Chang.*, 61, 102037,  
417 doi:https://doi.org/10.1016/j.gloenvcha.2020.102037, 2020.

418 Dullo, T. T., Darkwah, G. K., Gangrade, S., Morales-Hernández, M., Sharif, M. B., Kalyanapu, A. J., Kao, S. C., Ghafoor, S.  
419 and Ashfaq, M.: Assessing climate-change-induced flood risk in the Conasauga River watershed: An application of

ensemble hydrodynamic inundation modeling, *Nat. Hazards Earth Syst. Sci.*, 21(6), 1739–1757, doi:10.5194/nhess-21-1739-2021, 2021.

Fang, J., Lincke, D., Brown, S., Nicholls, R. J., Wolff, C., Merkens, J. L., Hinkel, J., Vafeidis, A. T., Shi, P. and Liu, M.: Coastal flood risks in China through the 21st century – An application of DIVA, *Sci. Total Environ.*, 704, 135311, doi:10.1016/j.scitotenv.2019.135311, 2020.

Fang, J., Wahl, T., Zhang, Q., Muis, S., Hu, P., Fang, J., Du, S., Dou, T. and Shi, P.: Extreme sea levels along coastal China: uncertainties and implications, *Stoch. Environ. Res. Risk Assess.*, 35(2), 405–418, doi:10.1007/s00477-020-01964-0, 2021.

Gori, A., Blessing, R., Juan, A., Brody, S. and Bedient, P.: Characterizing urbanization impacts on floodplain through integrated land use, hydrologic, and hydraulic modeling, *J. Hydrol.*, 568, 82–95, doi:10.1016/j.jhydrol.2018.10.053, 2019.

Gounaridis, D., Chorianopoulos, I., Symeonakis, E. and Koukoulas, S.: A Random Forest-Cellular Automata modelling approach to explore future land use/cover change in Attica (Greece), under different socio-economic realities and scales, *Sci. Total Environ.*, 646, 320–335, doi:10.1016/j.scitotenv.2018.07.302, 2019.

Hallegatte, S., Green, C., Nicholls, R. J. and Corfee-Morlot, J.: Future flood losses in major coastal cities, *Nat. Clim. Chang.*, 3(9), 802–806, doi:10.1038/nclimate1979, 2013.

Haynes, P., Hehl-Lange, S. and Lange, E.: Mobile Augmented Reality for Flood Visualisation, *Environ. Model. Softw.*, 109, 380–389, doi:10.1016/j.envsoft.2018.05.012, 2018.

He, C., Liu, Z., Wu, J., Pan, X., Fang, Z., Li, J. and Bryan, B. A.: Future global urban water scarcity and potential solutions, *Nat. Commun.*, 12(1), 1–11, doi:10.1038/s41467-021-25026-3, 2021.

Hoch, J. M., Eilander, D., Ikeuchi, H., Baart, F. and Winsemius, H. C.: Evaluating the impact of model complexity on flood wave propagation and inundation extent with a hydrologic-hydrodynamic model coupling framework, *Nat. Hazards Earth Syst. Sci.*, 19(8), 1723–1735, doi:10.5194/nhess-19-1723-2019, 2019.

Hunt, A. and Watkiss, P.: Climate change impacts and adaptation in cities: A review of the literature, *Clim. Change*, 104(1), 13–49, doi:10.1007/s10584-010-9975-6, 2011.

Huong, H. T. L. and Pathirana, A.: Urbanization and climate change impacts on future urban flooding in Can Tho city, Vietnam, *Hydrol. Earth Syst. Sci.*, 17(1), 379–394, doi:10.5194/hess-17-379-2013, 2013.

IPCC: Climate Change 2014: Impacts, Adaptation, and Vulnerability. Part A: Global and Sectoral Aspects. Contribution of Working Group II to the Fifth Assessment Report of the Intergovernmental Panel on Climate Change, Cambridge University Press, Cambridge, UK., 2014.

Kabat, P., Fresco, L. O., Stive, M. J. F., Veerman, C. P., van Alphen, J. S. L. J., Parmet, B. W. A. H., Hazeleger, W. and Katsman, C. A.: Dutch coasts in transition, *Nat. Geosci.*, 2(7), 450–452, doi:10.1038/ngeo572, 2009.

Kim, Y. and Newman, G.: Advancing scenario planning through integrating urban growth prediction with future flood risk models, *Comput. Environ. Urban Syst.*, 82, 101498, doi:https://doi.org/10.1016/j.compenvurbsys.2020.101498, 2020.

454 Kopp, R. E., DeConto, R. M., Bader, D. A., Hay, C. C., Horton, R. M., Kulp, S., Oppenheimer, M., Pollard, D. and Strauss,  
 455 B. H.: Evolving understanding of Antarctic ice-sheet physics and ambiguity in probabilistic sea-level projections, arXiv,  
 456 2017.

457 Lai, C., Shao, Q., Chen, X., Wang, Z., Zhou, X., Yang, B. and Zhang, L.: Flood risk zoning using a rule mining based on ant  
 458 colony algorithm, *J. Hydrol.*, 542, 268–280, doi:<https://doi.org/10.1016/j.jhydrol.2016.09.003>, 2016.

459 Liang, X., Liu, X., Li, X., Chen, Y., Tian, H. and Yao, Y.: Delineating multi-scenario urban growth boundaries with a CA-  
 460 based FLUS model and morphological method, *Landsc. Urban Plan.*, 177, 47–63,  
 461 doi:10.1016/j.landurbplan.2018.04.016, 2018.

462 Lin, W., Sun, Y., Nijhuis, S. and Wang, Z.: Scenario-based flood risk assessment for urbanizing deltas using future land-use  
 463 simulation (FLUS): Guangzhou Metropolitan Area as a case study, *Sci. Total Environ.*, 739, 139899,  
 464 doi:10.1016/j.scitotenv.2020.139899, 2020.

465 Liu, J., Kuang, W., Zhang, Z., Xu, X., Qin, Y., Ning, J., Zhou, W., Zhang, S., Li, R., Yan, C., Wu, S., Shi, X., Jiang, N., Yu,  
 466 D., Pan, X. and Chi, W.: Spatiotemporal characteristics, patterns and causes of land use changes in China since the late  
 467 1980s, *Dili Xuebao/Acta Geogr. Sin.*, 69(1), 3–14, doi:10.11821/dlxb201401001, 2014.

468 Liu, X., Liang, X., Li, X., Xu, X., Ou, J., Chen, Y., Li, S., Wang, S. and Pei, F.: A future land use simulation model (FLUS)  
 469 for simulating multiple land use scenarios by coupling human and natural effects, *Landsc. Urban Plan.*, 168, 94–116,  
 470 doi:10.1016/j.landurbplan.2017.09.019, 2017.

471 Muis, S., Güneralp, B., Jongman, B., Aerts, J. C. J. H. and Ward, P. J.: Flood risk and adaptation strategies under climate  
 472 change and urban expansion: A probabilistic analysis using global data, *Sci. Total Environ.*, 538, 445–457,  
 473 doi:10.1016/j.scitotenv.2015.08.068, 2015.

474 Muis, S., Verlaan, M., Winsemius, H. C., Aerts, J. C. J. H. and Ward, P. J.: A global reanalysis of storm surges and extreme  
 475 sea levels, *Nat. Commun.*, 7, 11969, doi:10.1038/ncomms11969, 2016.

476 Nithila Devi, N., Sridharan, B. and Kuiry, S. N.: Impact of urban sprawl on future flooding in Chennai city, India, *J. Hydrol.*,  
 477 574, 486–496, doi:10.1016/j.jhydrol.2019.04.041, 2019.

478 O’Loughlin, F. E., Neal, J., Schumann, G. J. P., Beighley, E. and Bates, P. D.: A LISFLOOD-FP hydraulic model of the  
 479 middle reach of the Congo, *J. Hydrol.*, 580, doi:10.1016/j.jhydrol.2019.124203, 2020.

480 Parodi, M. U., Giardino, A., Van Dongeren, A., Pearson, S. G., Bricker, J. D. and Reniers, A. J. H. M.: Uncertainties in  
 481 coastal flood risk assessments in small island developing states, *Nat. Hazards Earth Syst. Sci.*, 20(9), 2397–2414,  
 482 doi:10.5194/nhess-20-2397-2020, 2020.

483 Parris, A., Bromirski, P., Burkett, V., Cayan, D., Culver, M., Hall, J., Horton, R., Knuuti, K., Moss, R., Obeysekera, J.,  
 484 Sallenger, A. and Weiss, J.: Global Sea Level Rise Scenarios for the US National Climate Assessment, NOAA Tech  
 485 Memo OAR CPO, 1–37, doi:[https://scenarios.globalchange.gov/sites/default/files/NOAA\\_SLR\\_r3\\_0.pdf](https://scenarios.globalchange.gov/sites/default/files/NOAA_SLR_r3_0.pdf), 2012.

486 Pecl, G. T., Araújo, M. B., Bell, J. D., Blanchard, J., Bonebrake, T. C., Chen, I. C., Clark, T. D., Colwell, R. K., Danielsen,  
 487 F., Evengård, B., Falconi, L., Ferrier, S., Frusher, S., Garcia, R. A., Griffis, R. B., Hobday, A. J., Janion-Scheepers, C.,

488 Jarzyna, M. A., Jennings, S., Lenoir, J., Linnetved, H. I., Martin, V. Y., McCormack, P. C., McDonald, J., Mitchell, N.  
 489 J., Mustonen, T., Pandolfi, J. M., Pettorelli, N., Popova, E., Robinson, S. A., Scheffers, B. R., Shaw, J. D., Sorte, C. J.  
 490 B., Strugnell, J. M., Sunday, J. M., Tuanmu, M. N., Vergés, A., Villanueva, C., Wernberg, T., Wapstra, E. and  
 491 Williams, S. E.: Biodiversity redistribution under climate change: Impacts on ecosystems and human well-being,  
 492 *Science* (80-. ), 355(6332), doi:10.1126/science.aai9214, 2017.

493 Rajib, A., Liu, Z., Merwade, V., Tavakoly, A. A. and Follum, M. L.: Towards a large-scale locally relevant flood inundation  
 494 modeling framework using SWAT and LISFLOOD-FP, *J. Hydrol.*, 581, 124406, doi:10.1016/j.jhydrol.2019.124406,  
 495 2020.

496 Ramaswami, A., Russell, A. G., Culligan, P. J., Rahul Sharma, K. and Kumar, E.: Meta-principles for developing smart,  
 497 sustainable, and healthy cities, *Science* (80-. ), 352, 940–943, doi:10.1126/science.aaf7160, 2016.

498 Reckien, D., Salvia, M., Heidrich, O., Church, J. M., Pietrapertosa, F., De Gregorio-Hurtado, S., D’Alonzo, V., Foley, A.,  
 499 Simoes, S. G., Krkoška Lorencová, E., Orru, H., Orru, K., Wejs, A., Flacke, J., Olazabal, M., Geneletti, D., Feliu, E.,  
 500 Vasilie, S., Nador, C., Krook-Riekkola, A., Matosović, M., Fokaides, P. A., Ioannou, B. I., Flamos, A., Spyridaki, N.  
 501 A., Balzan, M. V., Fülöp, O., Paspaldzhiev, I., Grafakos, S. and Dawson, R.: How are cities planning to respond to  
 502 climate change? Assessment of local climate plans from 885 cities in the EU-28, *J. Clean. Prod.*, 191, 207–219,  
 503 doi:10.1016/j.jclepro.2018.03.220, 2018.

504 Song, J., Fu, X., Wang, R., Peng, Z.-R. and Gu, Z.: Does planned retreat matter? Investigating land use change under the  
 505 impacts of flooding induced by sea level rise, *Mitig. Adapt. Strateg. Glob. Chang.*, 23(5), 703–733,  
 506 doi:10.1007/s11027-017-9756-x, 2018.

507 Sosa, J., Sampson, C., Smith, A., Neal, J. and Bates, P.: A toolbox to quickly prepare flood inundation models for  
 508 LISFLOOD-FP simulations, *Environ. Model. Softw.*, 123, 104561, doi:https://doi.org/10.1016/j.envsoft.2019.104561,  
 509 2020.

510 Sun, L., Chen, J., Li, Q. and Huang, D.: Dramatic uneven urbanization of large cities throughout the world in recent decades,  
 511 *Nat. Commun.*, 11(1), 5366, doi:10.1038/s41467-020-19158-1, 2020.

512 Tessler, Z. D., Vorosmarty, C. J., Grossberg, M., Gladkova, I., Aizenman, H., Syvitski, J. P. M. and Foufoula-Georgiou, E.:  
 513 Profiling risk and sustainability in coastal deltas of the world, *Science* (80-. ), 349, 638–643,  
 514 doi:10.1126/science.aab3574, 2015.

515 United Nations: Factsheet: People and oceans., 2017.

516 United Nations: 2018 Revision of World Urbanization Prospects. [online] Available from: <https://population.un.org/wup/>,  
 517 2018.

518 Vousdoukas, M. I., Mentaschi, L., Voukouvalas, E., Verlaan, M., Jevrejeva, S., Jackson, L. P. and Feyen, L.: Global  
 519 probabilistic projections of extreme sea levels show intensification of coastal flood hazard, *Nat. Commun.*, 9(1), 1–12,  
 520 doi:10.1038/s41467-018-04692-w, 2018.



521 Wang, Z., Lai, C., Chen, X., Yang, B., Zhao, S. and Bai, X.: Flood hazard risk assessment model based on random forest, *J.*  
522 *Hydrol.*, 527, 1130–1141, doi:10.1016/j.jhydrol.2015.06.008, 2015.

523 Wing, O. E. J., Sampson, C. C., Bates, P. D., Quinn, N., Smith, A. M. and Neal, J. C.: A flood inundation forecast of  
524 Hurricane Harvey using a continental-scale 2D hydrodynamic model, *J. Hydrol. X*, 4, 100039,  
525 doi:https://doi.org/10.1016/j.hydroa.2019.100039, 2019.

526 Xian, S., Yin, J., Lin, N. and Oppenheimer, M.: Influence of risk factors and past events on flood resilience in coastal  
527 megacities: Comparative analysis of NYC and Shanghai, *Sci. Total Environ.*, 610–611, 1251–1261,  
528 doi:10.1016/j.scitotenv.2017.07.229, 2018.

529 Xu, K., Fang, J., Fang, Y., Sun, Q., Wu, C. and Liu, M.: The Importance of Digital Elevation Model Selection in Flood  
530 Simulation and a Proposed Method to Reduce DEM Errors: A Case Study in Shanghai, *Int. J. Disaster Risk Sci.*,  
531 doi:10.1007/s13753-021-00377-z, 2021.

532 Xu, W. (Ato) and Yang, L.: Evaluating the urban land use plan with transit accessibility, *Sustain. Cities Soc.*, 45, 474–485,  
533 doi:10.1016/j.scs.2018.11.042, 2019.

534 Xu, X., Liu, J., Zhang, Z., Zhou, W., Zhang, S., Li, R., Yan, C., Wu, S. and Shi, X.: A Time Series Land Ecosystem  
535 Classification Dataset of China in Five-Year Increments (1990–2010), *J. Glob. Chang. Data Discov.*, 1(1), 52–59,  
536 doi:10.3974/geodp.2017.01.08, 2017.

537 Yin, J., Yu, D., Yin, Z., Wang, J. and Xu, S.: Modelling the combined impacts of sea-level rise and land subsidence on storm  
538 tides induced flooding of the Huangpu River in Shanghai, China, *Clim. Change*, 119(3–4), 919–932,  
539 doi:10.1007/s10584-013-0749-9, 2013.

540 Yin, J., Jonkman, S., Lin, N., Yu, D., Aerts, J., Wilby, R., Pan, M., Wood, E., Bricker, J., Ke, Q., Zeng, Z., Zhao, Q., Ge, J.  
541 and Wang, J.: Flood Risks in Sinking Delta Cities: Time for a Reevaluation?, *Earth’s Futur.*, 8(8),  
542 doi:10.1029/2020EF001614, 2020.

543 Zhai, Y., Yao, Y., Guan, Q., Liang, X., Li, X., Pan, Y., Yue, H., Yuan, Z. and Zhou, J.: Simulating urban land use change by  
544 integrating a convolutional neural network with vector-based cellular automata, *Int. J. Geogr. Inf. Sci.*, 34(7), 1475–  
545 1499, doi:10.1080/13658816.2020.1711915, 2020.

546 Zhao, G., Bates, P. and Neal, J.: The Impact of Dams on Design Floods in the Conterminous US, *Water Resour. Res.*, 56(3),  
547 1–15, doi:10.1029/2019WR025380, 2020.

548 Zhao, L., Song, J. and Peng, Z.-R.: Modeling Land-Use Change and Population Relocation Dynamics in Response to  
549 Different Sea Level Rise Scenarios: Case Study in Bay County, Florida, *J. Urban Plan. Dev.*, 143(3), 04017012,  
550 doi:10.1061/(asce)up.1943-5444.0000398, 2017.

551 Zhou, L., Dang, X., Sun, Q. and Wang, S.: Multi-scenario simulation of urban land change in Shanghai by random forest and  
552 CA-Markov model, *Sustain. Cities Soc.*, 55, 102045, doi:10.1016/j.scs.2020.102045, 2020.

553 Zhou, Q., Leng, G., Su, J. and Ren, Y.: Comparison of urbanization and climate change impacts on urban flood volumes:  
554 Importance of urban planning and drainage adaptation, *Sci. Total Environ.*, 658, 24–33,  
555 doi:<https://doi.org/10.1016/j.scitotenv.2018.12.184>, 2019.

556 Xu, X.: China GDP Spatial Distribution Kilometer Grid Dataset [dataset], <http://www.resdc.cn/DOI/doi.aspx?DOIid=33>,  
557 2017a.

558 Xu, X.: China Population Spatial Distribution Kilometer Grid Dataset [dataset],  
559 <http://www.resdc.cn/DOI/DOI.aspx?DOIid=32>, 2017b.